Electric Analog Studies of Flow to Wells in the Punjab Aquifer of West Pakistan

GEOLOGICAL SURVEY WATER-SUPPLY PAPER 1608–N

Prepared in cooperation with the West Pakistan Water and Power Development Authority under the auspices of the U.S. Agency for International Development

Electric Analog Studies of Flow to Wells in the Punjab Aquifer of West Pakistan

By M. J. MUNDORFF, G. D. BENNETT, *and* MASOOD AHMAD

CONTRIBUTIONS TO THE HYDROLOGY OF ASIA AND OCEANIA

GEOLOGICAL SURVEY WATER-SUPPLY PAPER 1608-N

Prepared in cooperation with the West Pakistan Water and Power Development Authority under the auspices of the U.S. Agency for International Development

UNITED STATES GOVERNMENT PRINTING OFFICE, WASHINGTON : 1972

UNITED STATES DEPARTMENT OF THE INTERIOR

ROGERS C. B. MORTON, *Secretary*

GEOLOGICAL SURVEY

V. E. McKelvey, *Director*

Library of Congress catalog-card No. 74–188320

For sale by the Superintendent of Documents, U.S. Government Printing Office
Washington, D.C. 20402 (paper cover)
Stock Number 2401–0257

CONTENTS

ILLUSTRATIONS

TABLES

CONTRIBUTIONS TO THE HYDROLOGY OF ASIA AND OCEANIA

ELECTRIC ANALOG STUDIES OF FLOW TO WELLS IN THE PUNJAB AQUIFER OF WEST PAKISTAN

By M. J. MUNDORFF, G. D. BENNETT, and MASOOD AHMAD

ABSTRACT

A series of experiments was performed with a steady-state electric analog simulating a cylindrical segment of the aquifer underlying the plains of the Punjab region of West Pakistan. In most of the experiments recharge was assumed to be from the surface, within a specified radius of influence, and distributed uniformly over the area within this radius. Experiments were made with different anisotropies (ratios of lateral to vertical resistance) so that various possible combinations of aquifer thickness and effective radius or radius of influence and combinations of lateral and vertical permeability could be included in the models. Flow nets were constructed to show distribution of potential in the vertical section and intersections of stream surfaces with the vertical plane.

The series of experiments in which the screened interval is in the upper part of the aquifer shows that flow decreases and stream tubes shift progressively toward the upper part of the aquifer as anisotropy increases. Another series illustrates that total yield increases and yield per foot of screen decreases as screen length increases.

The experiments indicate that, under conditions prevalent in the Punjab, the distance-drawdown method for determining permeability gives results with an error of 10 percent or less provided that at least one piezometer or observation well is within a few feet of the pumped well and that no observation well or piezometer used is more than 100 feet from the pumped well.

Relative traveltime for each of 10 stream tubes is given for three models. Relative traveltimes for one-fourth and one-half the effective radius are given for selected stream tubes. By substituting values for the aquifer parameters, actual traveltimes are computed from the relative-traveltime data.

INTRODUCTION

PURPOSE AND SCOPE OF REPORT

The upper Indus plain, a triangular area of some 40,000–50,000 sq mi (square miles), extends north and northeast from the junc-

tion of the Indus and Panjnad-Sutlej Rivers in the Punjab region of West Pakistan. This plain, containing the largest contiguous irrigated area in the world, is underlain by a thick sequence of alluvial deposits that composes a tremendous aquifer system. The alluvium, presumably chiefly of fluviatile origin, consists of lenticular bodies, lenses, and stringers of fine to medium sand, silt, and clay. Most recharge to the aquifer is from an extensive ramified canal system. Because of the gradual slopes, generally 1–1½ feet per mile, the drainage is poor. Over much of the area large seepage losses from the irrigation channels have caused the water table to rise within a few feet of the surface. At the same time, the quantities of water actually reaching the fields have been inadequate for both optimal crop development and proper leaching, and large tracts of land have become salinized. The problems in the Indus plains, therefore, involve insufficient water for leaching and crop growth and a high water table. The logical solution to these problems, the one adopted by the West Pakistan Water and Power Development Authority (WAPDA), is to obtain additional water supplies by developing the vast aquifer underlying the plain through the use of tubewell[1] networks.

The Water and Soils Investigation Divisions (WASID) of WAPDA has drilled more than 1,000 test wells and made more than 150 aquifer tests to obtain data on the nature, extent, and hydraulic characteristics of the aquifer and on the ground-water quality. These invtstigations were supported by a program of the U.S. Agency for International Development which provided advisors from the U.S. Geological Survey as well as essential equipment and supplies.

The field investigations were supplemented by electric analog studies of selected hydrologic problems. The general objective of this analog study reported herein was to achieve a better understanding of the ground-water system in the vicinity of discharging wells in the upper Indus plain. More specifically, the objectives were to determine: (1) the amount of time for water particles to flow from various points of origin to the well screen, (2) the degree of brackish-water intrusion from below, well depths and degrees of anisotropy being variables, (3) the effect of low-permeability layers on the flow pattern, (4) the errors which, in the computation of permeabilities from aquifer tests, are due to ver-

[1] "Tubewell" is a term used in India and Pakistan for a conventional drilled and screened well.

tical convergence of flow near the test well, and (5) the optimal location of observation wells to minimize these errors.

ACKNOWLEDGMENTS

The authors are indebted to several officers of WASID for their assistance in completing the analog study. The support of Mr. S. M. Said, Chief Engineer, WASID, and Mr. M. A. Lateef, Superintending Hydrologist, General Hydrology Circle, WASID, is gratefully acknowledged.

AQUIFER CHARACTERISTICS

Generally, the alluvial deposits which underlie the plain compose a single anisotropic aquifer in which water-table conditions prevail. Locally, however, there are boundaries, barriers, and semiartesian flow conditions.

Fine- to medium-grained sand constitutes as much as 60–70 percent of the total material of the alluvial aquifer. Silt, clay, and mixtures of silt, clay, and fine sand in the form of lenticular bodies make up the remaining 30–40 percent. Gravel is rare. The lenses of finer grained, less permeable materials act as local boundaries or semiconfining layers. Near the central part of the plain is a number of fairly small bedrock hills which protrude through the alluvium to form local boundaries (Greenman and others, 1967, fig. 10). The tops of these hills are less than 1,000 feet below the land surface over an area of at least 400 sq mi; elsewhere the alluvium is known to be more than 1,000 feet thick and at places is more than 1,500 feet thick.

Lateral permeabilities of the screened interval, determined in 141 pumping tests, are chiefly in the range of 0.001–0.006 and average average 0.0032 cfs per sq ft (cubic feet per second per square foot) (Bennett and others, 1967). The aquifer is anisotropic. Vertical permeabilities, determined in 14 tests, are in the range of 0.00001–0.0004 and average about 0.00008 cfs per sq ft. The ratio of lateral permeability to vertical permeability therefore ranges from 3:1 to 200:1; most of the ratios are between 15:1 and 90:1, and the average is about 75:1. The vertical-permeability figures represent the average vertical permeability of the material between the water table and the top of the screened interval of the test well. However, the alluvium is made up of innumerable strata of varying degrees of permeability, and the vertical permeability of these individual layers may vary over an extremely wide range.

Most recharge to the aquifer is from leakage of the canal irrigation system; the rest of the recharge comes from seepage from irrigated fields and from rainfall. In nonpumped areas, discharge

is almost entirely by evapotranspiration, a process aided by the large amount of water surface area. On a map the irrigation system, which includes literally thousands of distributaries and field ditches, looks like a diagram showing the veins in a body. Thus, the ground-water movement in nonpumped areas is dominantly vertical. Under such conditions, the water flowing toward a newly pumped well first comes from storage. As the cone of depression expands, more and more sources of recharge are encompassed by the cone until equilibrium is reached, which is when most of the water entering the well is derived from vertical recharge.

In areas of ground-water development such as Salinity Control and Reclamation Project No. 1 (SCARP 1), it is apparent that recharge is dominantly vertical. In this area of 1.2 million acres, about 11 million acre-feet of water was pumped from about 2,150 project wells which had been operating for 4 years (July 1962–June 1966). More than 92 percent of this water was from recharge within the area, about 7 percent was from storage, and less than 1 percent was from lateral inflow. The average water-level decline within SCARP 1 during this 4-year period was about 5 feet. At least the interior wells in this gigantic well field derive their recharge entirely from vertical percolation that affects an area having a fairly small radius, perhaps 0.5–1 mile (there is roughly one well per square mile); thus, the aquifer approximates the steady-state condition. The experiments in this report were based on the assumption of conditions similar to those within SCARP 1: steady-state conditions, a cylindrical aquifer segment having a finite radius of influence, and, in most of the experiments, uniform vertical recharge over the area of influence.

MODEL DESIGN

The model selected was similar to the one described by Stallman (1963). Briefly, the model is based on an analogy between the flow of electricity through a resistance grid and the flow of water through an aquifer. A rectangular grid of resistors represents a cylindrical aquifer segment which has effective radius r_e, inner radius r_w, and saturated thickness m and lies above an impermeable layer. As this model consists only of resistors, it has no capacity for storage and, therefore, can only simulate the steady-state condition.

The flow toward the well, assumed to be symmetrical about the z axis, can be fully described in terms of the r and z coordinates in the cylindrical coordinate system. With this type of axial symmetry, cross-sectional areas for both lateral and vertical flow expand continuously as distance from the vertical axis increases.

Thus there is a regular decrease in hydraulic resistance as radial distance from the well increases. The analog model used in these studies is a two-dimensional network of resistors which represents the r–z plane. To account for the decreasing hydraulic resistance, a logarithmic scale of distance is used along the radial axis, and the electrical-resistance values, employed in successive vertical rows of the network, are varied through a regularly decreasing sequence.

An excellent theoretical development of the analog relations is given by Stallman (1963). Although repetition of this material would be redundant, an alternative approach may interest some readers; therefore, a somewhat less rigorous development of the analog relations is outlined here. This development depends upon the consideration of the functions of individual resistance elements in simulating segments of the aquifer. The concept of the hydraulic resistance of an aquifer segment to flow in a given direction is also utilized. If the area of an aquifer segment normal to a given direction is A, its thickness parallel to that direction is 1, and its permeability to flow in that direction is P, then its hydraulic resistance to flow in this direction is given by

$$H=\frac{1}{PA}. \tag{1}$$

The analogy between this hydraulic resistance and electrical resistance is obvious.

Each junction of the model corresponds to a point in the r–z plane of the aquifer. The points represented by the junctions are uniformly spaced in the vertical direction; that is, parallel to the z axis, the points represented by successive junctions occur at equally spaced intervals, Δz. Parallel to the r axis, the radii represented by successive junctions are spaced in such a way that the change in the logarithm of r between successive junctions remains the same. Thus the radius represented by each junction is a constant multiple, α, of that represented by the preceding junction inward. If the junctions along the r axis are numbered, beginning with $n=0$ at the well radius, r_w, the radii represented by successive junctions fall in the series $\alpha^0 r_w$, αr_w, $\alpha^2 r_w \ldots \alpha^n r_w \ldots$.

The function of the lateral resistors may be visualized by imagining that the aquifer is divided into a series of coaxial cylindrical shells in such a way that the outer radius of each is this constant multiple, α, of its inner radius. These shells intersect the r–z plane as a series of rectangles, such as ABCD in figure 1, which represents the intersection with the r–z plane of an aquifer shell extending from an inner radius of $\alpha^{n-1} r_w$ to an outer radius $\alpha^n r_w$.

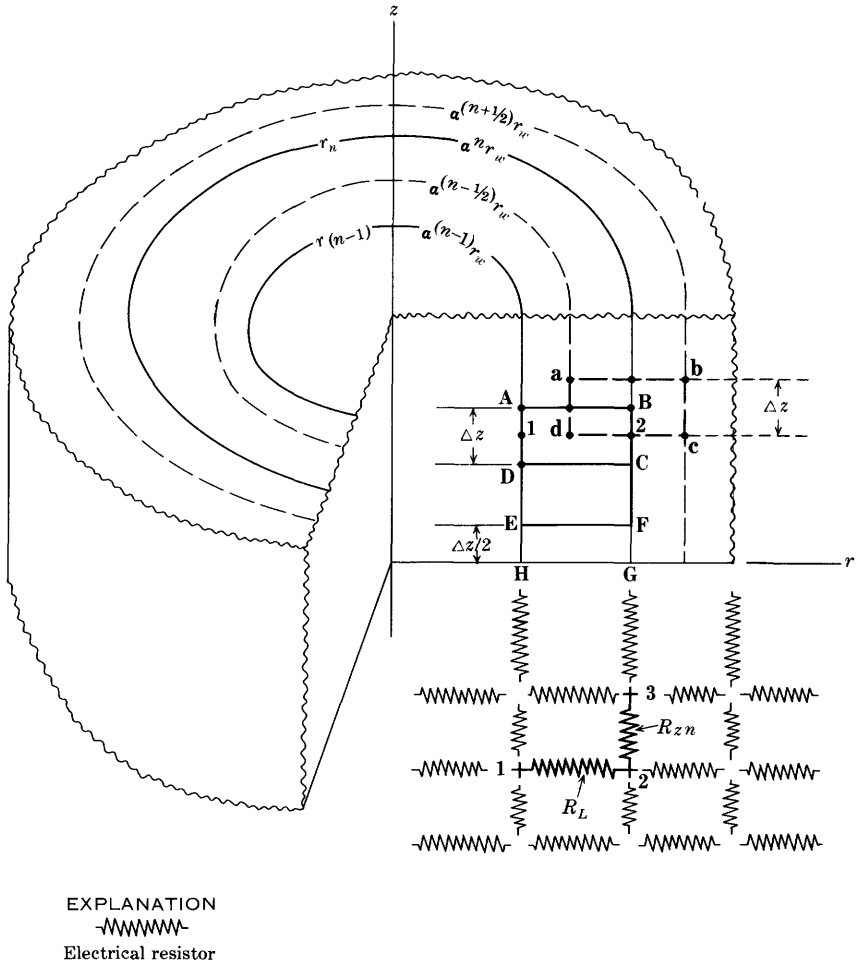

FIGURE 1.—Aquifer segments represented by lateral- and vertical-resistance elements.

ABCD, an interior shell, has a thickness, Δz, equal to $m/(f-1)$, where m is the thickness of the subject aquifer and f is the number of lateral rows in the analog network. The uppermost and lowermost shells have a thickness $\Delta z/2$, as represented by the rectangle EFGH in figure 1.

The hydraulic resistance of the aquifer shell ABCD is calculated by dividing it into a series of infinitesimal shells having radial width dr and cross-sectional area $2\pi r\Delta z$. The hydraulic resistance of one of these elements will be $dr/(P_L 2\pi r\Delta z)$, where P_L is the lateral permeability. The hydraulic resistance of the shell repre-

sented by ABCD in figure 1 is obtained by summing these infinitesimal terms as resistances in series:

$$H_L = \int_{r=\alpha^{n-1}r_w}^{r=\alpha^n r_w} \frac{dr}{P_L 2\pi r \Delta z} = \frac{\ln \alpha}{2\pi P_L \Delta z}, \tag{2}$$

where H_L denotes the required lateral hydraulic resistance.

This hydraulic resistance is represented by the electrical resistance R_L, extending between junctions 1 and 2 of the analog network in figure 1. The electrical resistance is proportional to the hydraulic resistance:

$$R_L = \frac{k \ln \alpha}{2\pi P_L \Delta z}, \tag{3}$$

where k is a constant of proportionality. If the model equifer is made up of a succession of shells having radii in the series $\alpha^0 r_w$, αr_w, $\alpha^2 r_w \ldots \alpha^n r_w \ldots$, the hydraulic resistance of each is given by equation 2, as the logarithmic term is the same for each; the electrical resistance used to represent each shell is given by equation 3. Thus, the model design incorporates the same resistance throughout the interior lateral rows, and successive junctions along these rows represent radii in the previously defined series.

The uppermost and lowermost shells, such as those represented by the rectangle EFGH in figure 1, are only half as thick as the interior shells. The resistance used in the uppermost and lowermost lateral rows of the network is thus twice that used in the interior rows.

To visualize the function of the vertical resistors of the network, consider the vertical resistance connected between junctions 2 and 3 in figure 1. The radius represented by these junctions is r_n or $\alpha^n r_w$; the resistor simulates the hydraulic resistance of a cylindrical aquifer shell which extends from an inner radius $\alpha^{n-\frac{1}{2}}$ to an outer radius $\alpha^{n+\frac{1}{2}}$ and has a height Δz. The rectangle abcd in figure 1 represents the intersection of this shell with the r–z plane. If α is close to unity, the arithmetic mean of the inner and outer radii of this aquifer shell is approximately r_n or $\alpha^n r_w$, and the cross-sectional area for vertical flow is $2\pi r_n (\Delta r)_n$, where $(\Delta r)_n$ is the radial width. This radial width is approximately $r_n \Delta (\ln r)_n$, where $\Delta (\ln r)_n$, the change in $\ln r$ between the inner and outer radial boundaries of the shell, is equal to $\ln \alpha$. The cross-sectional area for vertical flow may therefore be expressed as $2\pi r^2 \ln \alpha$, and the vertical hydraulic resistance of the shell is given by

$$H_{zn} = \frac{\Delta z}{2\pi P_z r_n^2 \ln \alpha}, \tag{4}$$

where H_{zn} is the required hydraulic resistance and P_z is the vertical permeability of the aquifer.

The electrical resistances employed in the row at r_n are related to the vertical hydraulic resistance by the constant of proportionality used in equation 3:

$$R_{zn}=kH_{zn}=\frac{k\Delta z}{2\pi P_z r_n^2 \ln \alpha}, \tag{5}$$

where R_{zn} is the required vertical electrical resistance.

Owing to the reduced base areas of the innermost and outermost aquifer shells, the resistances used in the innermost and outermost vertical rows have higher values than those derived from equation 5. The outermost shell is terminated at r_e; that is, it extends from an inner radius $\alpha^{j-\frac{1}{2}}r_w$ to an outer radius $\alpha^j r_w$, where $\alpha^j=r_e/r_w$, rather than to an outer radius $\alpha^{j+\frac{1}{2}}r_w$. The innermost shell commences at the inner radius r_w; that is, it extends from an inner radius $\alpha^0 r_w$, rather than from an inner radius $\alpha^{-\frac{1}{2}}r_w$, to an outer radius $\alpha^{\frac{1}{2}}r_w$. The resistance, as given by equation 5, is multiplied by $(\alpha^2-1)/(\alpha-1)$ for the outermost vertical row and by $(\alpha+1)/\alpha$ for the innermost row.

From equation 5, the ratio of the resistances used in successive interior vertical rows (more specifically, the ratio of the resistances used for r_n, or $\alpha^n r_w$, to those used for r_{n-1}, or $\alpha^{n-1}r_w$) is

$$\frac{R_{zn}}{R_{z(n-1)}}=\frac{r_{(n-1)}^2}{r_n^2}=\frac{1}{\alpha^2}. \tag{6}$$

If equations 3 and 5 are combined, the ratio of the resistance used in the vertical row at r_n to the resistance used in the interior lateral rows throughout the model is

$$\frac{R_{zn}}{R_L}=\frac{P_L(\Delta z)^2}{P_z(r_n \ln \alpha)^2}. \tag{7}$$

The fact that equation 7 is equivalent to Stallman's equation 12, shows that models representing more than one aquifer situation may have the same design or that a single model may be used to represent a number of different aquifer situations, provided that the value of $P_L(\Delta z)^2/[P_z(r_n \ln \alpha)^2]$ is the same for each case. For example, suppose that a model is constructed in which $\alpha=1.65$, so $\ln \alpha$ is approximately 0.50, and that the ratio R_z/R_L is unity at a certain row. If the radius at this vertical row is 1,100 and Δz is 100, the model represents an aquifer for which P_L/P_z is approximately 33. However, if the radius at this row is 150 and Δz is 50, the model represents an aquifer for which P_L/P_z is approximately 2.25, and so on. It should be noted, of course, that such changes in

the radius represented by a given row produce proportional changes in r_w and r_e and that changes in Δz produce proportional changes in m. Thus while a given model may represent any anisotropy, the geometry of the well and aquifer for each case will differ. The principles outlined here are actually an expression of the familiar coordinate transformation used in the solution of problems involving anisotropic media; perhaps this is more apparent when the expression $(r_n \ln \alpha)^2$ from equation 7 is replaced by the equivalent expression $(\Delta r_n)^2$. On the basis of such principles, a given model network can represent any aquifer for which $(m/r_e)\sqrt{P_L/P_z}$ has a particular value. This quantity, termed the model constant and designated "C" in this paper, indicates the conditions to which the various experimental results are applicable. Altering the anisotropy represented by an analog network without changing the geometry of the subject system is accomplished by adding vertical rows at one side of the model and removing an equal number from the other side. For example, suppose a certain resistance, R_1, occurs in the vertical row at $n=10$ in a network representing a particular anisotropy. If a vertical row is added at the inner (r_w) side of the model and a row is removed from the outer (r_e) side, the resistance R_1 occurs at $n=11$. If the new network represents a system which has the same radius of influence, well radius, and aquifer thickness as the original network, the anisotropy P_L/P_z of the new network is α^2 times that of the original network. This relationship is easily demonstrated by applying equation 7 to the two cases and using $\alpha^{2n} r_w^2$ in place of r_n^2.

In addition to the model constant, certain factors relating to the screen geometry must be specified to describe the aquifer-well systems represented by a given model. It is convenient to take the base of the aquifer as the elevation datum and to indicate elevation as a dimensionless fraction, z/m, of the aquifer thickness. Similarly, it is convenient to indicate radial distance as a dimensionless fraction, r/r_e, of the radius of influence. The screen geometry represented by a given model experiment may then be described by stating the fractional elevations of the top and bottom of the screen (or screens) and the fractional radius, r_w/r_e, of the screen.

The model constant and screen geometry, though they describe the aquifer-well system represented by a given network, do not indicate the recharge (inflow) conditions of the system. These conditions, determined by the potential boundaries (current inputs) that are employed in each experiment, must be specified

as additional boundary conditions relating to the particular experiment.

In this model, the value of α was $\sqrt{2}$. This design proved convenient in that anisotropy could be changed by a factor of two by removing a vertical row from one side of the network and adding a row at the other. This design also permitted a sufficient density of junctions, and therefore of potential readings, which allowed ready construction of flow lines and lines of equal head throughout the system. Owing to the value of α used in the network, resistances in adjacent interior vertical rows differed by a factor of two.

Eleven lateral rows were used in the construction of the model. The nine interior rows represented aquifer segments of thickness $\Delta z = m/10$, and the uppermost and lowermost rows represented segments of thickness $\Delta z/2$ or $m/20$. A resistance of 1,000 ohms was used in the interior lateral rows.

The model was altered a number of times to represent different values of the model constant; however, the ratio of r_w to r_e was kept the same in most of the experiments. Most of the networks included approximately 240 junction points. As commercial resistors are not available for all values, it was not possible to build the grid exactly according to the specific values indicated by the equations. But the differences were small and did not significantly affect the results.

In some experiments, a layer of clay or other low-permeability material was simulated by increasing the vertical resistances at a particular level across the network. Each resistance in the high-resistance layer was increased to approximately 60 times the value indicated by the design equations. Because the lateral resistors were not modified in connection with this clay simulation, the "clay" models actually simulated a fairly thin layer of very low permeability material, and the vertical hydraulic resistance could increase without producing a significant effect upon the lateral hydraulic resistance. The high resistance interval, for example, could include a clay of thickness $m/50$ and have a vertical permeability approximately 0.0033 times that elsewhere in the aquifer.

OPERATION OF THE MODEL

A steady-state analog model analyzer of the type developed by the U.S. Geological Survey was used to supply power to the model and to measure the current and potential at various points.

Current was withdrawn through a wire, connected at r_w, to the lateral rows representing the screened interval. The screen terminal was connected to the ground of the power supply, so that

the screen potential was always zero. In the models in which uniform recharge to the water table was simulated, current inputs were made at selected junctions in the uppermost row of the model, usually at $n=18$, 20, 21, 22, and 23, except where more than 23 vertical rows were used. Inputs at these junctions were adjusted in proportion to the extent of aquifer surface area represented by the electrical elements at the junction. Owing to this input pattern, which simulated a uniform recharge per unit area over the region of influence of the well, the maximum potential occurred at $z/m=1.0$ and $r/r_e=1.0$. In experiment 14, current input was made through a vertical wire which was connected to each lateral row along one side of the model; thus flow from a radial boundary concentric to the well was simulated. Potential measurements were made at the various model junctions in each experiment. As both resistance values and potential differences were then known throughout the model, a complete plot of flux and potential could be made.

Data for the experiments are given in table 1. The first five columns give data essential to defining the parameters of each experiment. The last three columns give various possible anisotropy-dimension combinations applicable to each experiment. Flow nets, shown on plate 1, were drawn at a ratio of $m/r_e=0.173$ and could represent an aquifer segment 500 feet thick, having an effective radius of 2,896 feet and an r_w of 1.0 foot, or an aquifer segment 1,000 feet thick, having an effective radius of 5,792 feet and an r_w of 2.0 feet, and so on.

The top edge of the resistor grid represents the water table. In the aquifer, a cone of depression in the water table forms during pumping, so that the fractional elevation of the free surface varies from 1.0 at r_e to some lower elevation at r_w. Theoretically, the top of the resistance grid should be cut away toward r_w to simulate the thinning of the saturated aquifer thickness in that direction. In the Indus plains the drawdown of the free surface at r_w is rarely more than 3 or 4 feet, a fraction of 1 percent of the total aquifer thickness. However, the removal of a single lateral row, which simulates an aquifer segment of thickness $\Delta z=m/10$, would represent a drawdown of 50 or 100 feet; therefore, no reduction of the grid to simulate water-table drawdown was attempted.

FLOW PATTERNS

With the exception of experiment 14 (plate 1*B*) the maximum potential in all flow nets occurred on the water table at r_e. In experiment 14, which simulated flow from a radial boundary

TABLE 1.—*Analog model experiments*

[Model constant, $C=m/r_e\sqrt{P_L/P_z}$. Italicized possible anisotropy-dimension combinations are the true-to-scale combinations illustrated on pl. 1]

Model constant, C	Experiment	Plate 1—	r_e/r_w	Screen interval z/m	Possible anisotropy-dimension combinations: Anistropy P_L/P_z	m/r_e	Some possible values of m and r_e, given as m/r_e	
Uniform areal input								
1.380	8	*A*	2,896	0.55–0.85	*64:1*	*0.173*	*500/2,896,*	*1,000/5,792*
					32:1	.244	1,000/4,096,	708/2,896
					16:1	.345	1,000/2,896	
.977	15	*B*	2,896	.65– .85	64:1	.122	500/4,096,	354/2,896
					32:1	*.173*	*500/2,896,*	*1,000/5,792*
					16:1	.244	708/2,896	1,000/4,096
					8:1	.345	1,000/2,896	
.690	1	*A*	2,896	.55– .85	64:1	.086	250/2,896,	500/5,792
					32:1	.122	250/2,048,	500/4,096
					16:1	*.173*	*500/2,896,*	*1,000/5,792*
					8:1	.244	500/2,048	1,000/4,096
					4:1	.345	1,000/2,896	
.690	1A	*B*	2,896	.15– .45	(1)	(1)	(1)	(1)
.690	1C	*B*	2,896	.85– .95	(1)	(1)	(1)	(1)
.690	2	*D*	2,896	.65– .85	(2)	(2)	(2)	(2)
.489	7A1	None	2,896	.85– .95	32:1	.086	250/2,896	
.489	7F	None		.75– .85	16:1	.122	500/4,096	
.489	7E	*C*		.65– .85	*8:1*	*.173*	*500/2,896*	
.489	7A	*C*		.55– .85	4:1	.244	500/2,048,	1,000/4,096
.489	7D	*C*		.45– .85				
.489	7C	*C*		.35– .85	16:1	.086	250/2,896	
.489	7B	*C*		.25– .85	8:1	.122	500/4,096	
.345	7	*A*	2,896	.55– .85	*4:1*	*.173*	*500/2,896*	
					2:1	.244	708/2,896,	1,000/4,096
					1:1	.345	1,000/2,896	
.345	3	*D*	5,792	.55– .85	(3)	(3)	(3)	(3)
.345	4	*D*	2,896	.55– .85	(4)	(4)	(4)	(4)
.173	6	*A*	2,896	.55– .85	4:1	.086	250/2,896	
					2:1	.122	500/4,096	
					1:1	*.173*	*500/2,896*	
.173	5	*D*	2,896	.55– .85	(5)	(5)	(5)	(5)
Radial input								
0.690	14	*B*	2,896	.55–0.85	32:1	0.122	500/4,096	
					16:1	*.173*	*500/2,896*	
					8:1	.244	100/4,096	

[1] Same combinations as those in experiment 1.

[2] Same combinations as those in experiment 1, except for the clay layer at the bottom of the screen.

[3] Same combinations as those in experiment 7, except for the clay layer at the bottom of the screen. Note different ratio r_e/r_w.

[4] Same combinations as those in experiment 7, except for the clay layer at the bottom of the screen.

[5] Same combinations as those in experiment 6, except for the clay layer at the bottom of the screen.

coaxial with the well, this entire outer surface was at the maximum potential. The minimum potential in all experiments was at the contact simulating the screen. Lines of equipotential, based on the percentage of the total potential difference, were drawn, the maximum potential in the model being 100 percent. These percentages actually represent values of $[(h-h_w)/(h_o-h_w)]\times 100$,

where h is the head along the equipotential in question, h_w is the head in the well, and h_o is the head on the water table at r_e. Streamlines were also drawn on each flow net. To construct these streamlines, the currents through the lateral resistors between consecutive radii (between $\alpha^{-1}r_w$ and $\alpha^n r_w$) and the fraction of the total model current carried by each resistor were calculated. These fractions indicate the distribution of flow (stream-function) values along the vertical at $\alpha^{n-\frac{1}{2}}r_w$. If this distribution is determined for several values of n, streamlines can be constructed throughout the r–z plane. Nine streamlines, drawn on each flow net, divide the flow into 10 equal parts which represent increments of 0.1 in the stream function. On most flow nets an additional streamline (dashed), which indicates the stream function of 0.99, separates the 99 percent of the flow above the line from the 1 percent between the line and the base of the aquifer. On plate 1*C*, experiment 7A, dashed streamlines are shown for stream-function values of 0.95, 0.97, 0.98 and 0.99. On each flow net the scales along the vertical and radial axes, divided into tenths, indicate values of z/m and r/r_e respectively.

The four flow nets illustrated on plate 1*A*, cover the range of model constants, from 0.1726 to 1.380, the entire range encompassed by the series of experiments. In each of the four flow nets, the screened interval is from $z/m=0.55$ to $z/m=0.85$ ($z/m=0$ is the base of the aquifer). If $m/r_e=0.173$, the flow nets can represent aquifers 500 feet thick, having an r_e of 2,896 feet and an r_w of 1 foot and screened from 75 to 225 feet below the water table, or aquifers 1,000 feet thick, having an r_e of 5,792 feet and an r_w of 2 feet and screened from 150 to 450 feet, and so on. At the ratio of m/r_e drawn on plate 1*A*, experiment 6 represents isotropic conditions; experiment 7, a 4:1 ratio of P_L to P_z; experiment 1, a 16:1 ratio; experiment 8, a 64:1 ratio. Experiment 15 (pl. 1*B*), because of its 32:1 ratio, fits into this series between experiments 6, 7, 1, and 8 but has a shorter screen section. The effect that anisotropy has on channeling the flow into the screened interval is clearly shown in this series of flow nets.

Experiments 1A and 1C (both on pl. 1*B*) employed the same grid as experiment 1, where the model constant was 0.690, but utilized different screen settings. Experiment 14 (plate 1*B*) represents a radial input coaxial with the well, at a radius r_x. Actually, the resistor network was extended to $n=27$, or, considering the fact that $r_w=1$ foot and $m=500$ feet, $r_x=11{,}584$ feet. Because the equipotential lines were vertical between $n=27$ and $n=23$, they were plotted for a potential of 100 percent at r_x. The similarity

in the flow patterns between r_w and $r/r_e=0.3$ is obvious for experiments 1 and 14 (pl. 1*A* and *B*) ; that is, regardless of whether the flow is radial in the classical concept of an infinite aquifer or is derived entirely from vertical recharge within an r_e of about six times aquifer thickness, the flow pattern in the vicinity of a pumped well is essentially the same.

Experiments 7A-7F, shown on plate 1*C* (7F is not shown), involve changes in flow patterns due to changes in screen length, all other factors remaining constant. This series illustrates the fact that the longer the screen, the greater is the percentage of total potential drop that is used in the aquifer some distance from the screen and the smaller is the percentage of potential remaining for utilization in the vicinity of the well screen. The yield per foot of screen therefore decreases as the screen length increases.

Data on total flow entering each section of the screened interval for experiments 7A-7F are given in table 2. Flow per unit screen length for 7B, which has a six-unit screen length, is about 77 percent of the flow per unit screen length of 7F, which has a one-unit screen length. Flow into each screen length (depth interval) for each experiment is shown in table 3. In all experiments the maximum flow is in the bottommost screen interval. This is logical, because the greatest unscreened aquifer thickness lies below the screen. The opposite condition frequently applies to the Punjab, where the upper part of the screen often yields the most

TABLE 2.—*Comparison of flow, experiments 7A–7F*

Experiment	Screen interval z/m		Screen length, in fractions of aquifer thickness m.	Total flow to screen		Average flow per unit screen length, in model units
	Top	Bottom		Milliampere reading	Model units[1]	
7F	0.85	0.75	0.1	0.80	634	634
7E	.85	.65	.2	1.42	1,142	571
7A	.85	.55	.3	2.00	1,627	542
7D	.85	.45	.4	2.55	2,092	523
7C	.85	.35	.5	3.00	2,512	502
7B	.85	.25	.6	3.80	2,920	486

[1] Calculated from percentage-potential readings on the network and appropriate resistance values.

TABLE 3.—*Flow, in model units, into successive depth intervals of screen, experiments 7A–7F*

Screen interval z/m	Experiment					
	7F	7E	7A	7D	7C	7B
0.85–0.75	634	568	542	525	514	504
.75– .65	.....	574	529	506	493	482
.65– .55	.....	.....	556	516	493	480
.55– .45	.....	.....	.....	535	496	474
.45– .35	.....	.....	.....	.....	516	474
.35– .25	.....	.....	.....	.....	.....	506

water per unit length. One possible explanation is that the material immediately below the screen may be of below-average permeability, as drilling is frequently terminated when a low-permeability layer is reached. Another possible explanation is that the lower part of the screen may not be as well developed as the upper part.

Data for total flow and flow per unit screen length for aquifer models of different anisotropy are given in table 4. The flow decreases 7 or 8 percent for each fourfold increase in anisotropy, from 1:11 to 4:1, to 16:1, to 64:1.

Experiments 2, 3, 4, and 5 (plate 1*D*) illustrate the effect of highly resistant or low-permeability layers at or below the bottom of the well screen, a rather common condition for tubewells in the Indus plains. The only difference between experiments 3 and 4 is the ratio r_e/r_w. The effect of the clay layer is similar to that of an impervious base, in that most of the flow is confined to the interval above the clay.

TABLE 4.—*Total flow and flow per unit screen length in models of different anisotropy*

Experiment	Anistropy P_L/P_z	Screen interval z/m	Screen length, in fractions of aquifer thickness m	Total flow, in model units	Average flow per unit screen length [1]	Percentage of highest flow in group
6	1:1	0.55–0.85	0.3	1,840	613	100
7	4:1	.55– .85	.3	1,710	572	93
7A	8:1	.55– .85	.3	1,618	543	89
1	16:1	.55– .85	.3	1,540	524	85
8	64:1	.55– .85	.3	1,425	475	77
7E	8:1	.65– .85	.2	1,140	570	100
15	32:1	.65– .85	.2	980	532	93
7A1	8:1	.85– .95	.1	630	630	100
1C	16:1	.85– .95	.1	580	598	95

[1] Corrected for differences in total potential drop.

ERRORS IN DETERMINING PERMEABILITY BY ANALYSIS OF DISTANCE-DRAWDOWN PUMPING TESTS

The test results were utilized to examine errors involved in lateral-permeability determination by the distance-drawdown procedure, in which the flow thickness is assumed equal to the screen length of the well. Owing to difficulties in obtaining time-drawdown results that were consistent with available data, the distance-drawdown technique was applied (Bennett and others, 1967) in the Punjab for the analysis of pumping tests. However, because the aquifer thickness, the anisotropy, and certain other factors are generally unknown, distance-drawdown results are also subject to considerable inaccuracy. Steady-state analog results provide a convenient method of estimating the magnitude of these

errors. The results appear to be directly applicable to the Punjab tests, as the range of radii of influence represented by the analog experiments includes that of the test wells. The range of anisotropy employed in the experiments agreed with that from the few vertical-permeability determinations that were possible in the field.

The analysis of a pumping test gives a transmissibility value; to compute the coefficient of permeability, a figure for the aquifer thickness involved in the flow of water to the well must be determined. Some hydrologists have tried to estimate aquifer thickness, or "effective thickness" (Arif, 1966), or have applied a correction for partial penetration (Chaudhari, 1966). However, estimation of aquifer thickness is difficult in the Punjab; and, as the pumped water is derived either from storage at the water table or from surface recharge within a finite radius of the well, the boundary conditions assumed in most time-drawdown methods are inapplicable. In applying the distance-drawdown technique, Bennett, Rehman, Sheikh, and Ali (1967) assumed that flow was dominantly lateral within the screened interval near the pumped well and used drawdowns in observation wells located between 100 and 400 feet from the pumped well to determine the average coefficient of permeability of the screened interval.

Examination of the flow nets on plate 1 shows that only near the tubewell is the entire discharge confined to lateral flow through the screened interval of the aquifer. However, as the degree of anisotropy increases, the distance from the tubewell to the boundary of the zone of essentially lateral flow increases. Figure 2 shows a plot of the percentage of the total flow within the screened interval versus radial distance from the well for selected experiments. The same m/r_e values and anisotropy ratios used for the flow nets were used to plot the graphs. The scale at the top of figure 2 gives r as a percentage of r_e, so that the graph for each flow-net constant can be used for any of the combinations shown for that constant in table 1 or any other combination with the same flow-net constant.

It is apparent from the analog results that the pattern of essentially lateral movement persists to somewhat greater radii in the stream tubes terminating in the central part of the screen than in the stream tubes terminating at the upper and lower extremities of the screen. The errors in determining lateral permeability depend on the degree of convergence in the stream tubes within which the head gradient is measured rather than on the fraction of the total flow occurring within the screened interval. These

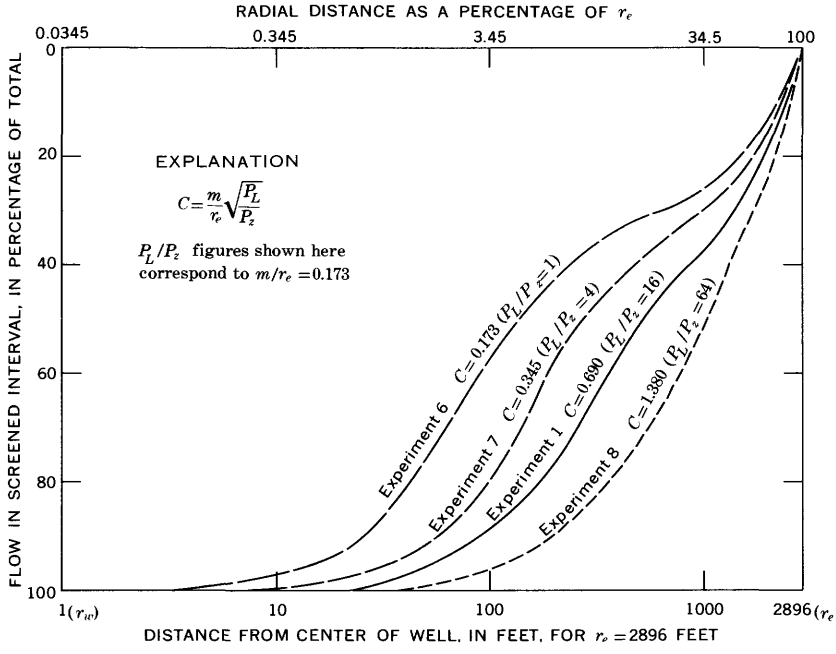

FIGURE 2.—Percentage of total flow within the screened interval at distance r from well.

errors were evaluated through study of the potential gradients observed in the analog network.

A semilogarithmic plot of drawdown versus distance is used for the distance-drawdown method of determining permeability. Distance from the pumped well is plotted on the logarithmic scale. In the analog model experiments, potentials were measured at 23 points between r_w and r_e along each horizontal. Where three lateral rows of resistors represented the screened interval, measurements along these rows represented potentials for the upper, center, and lower thirds of the screened interval, respectively. Semilog plots of potential along each row and of the average potential for all rows within the screened interval were made for most of the experiments. Selected profiles are shown in figures 3–7. In general, the potentials along the center of the screened interval plotted below the average graph, whereas the potentials along the upper and lower thirds plotted above the average graph. This is because there is considerable flow both above and below the screened interval that must be accommodated within the screened interval as r_w is approached. The result is that the potential gradient approaching the well is steeper in the lower and upper thirds than in the center third.

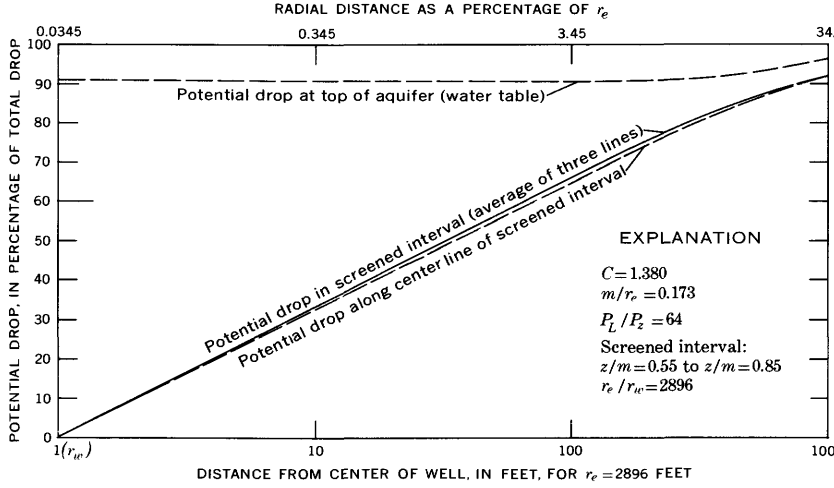

FIGURE 3.—Percentage of total potential drop within a given radius versus the radius, experiment 8.

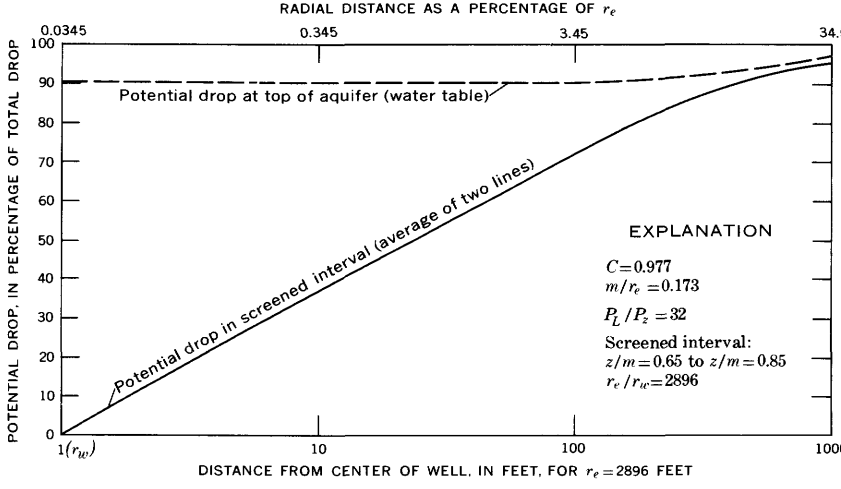

FIGURE 4.—Percentage of total potential drop within a given radius versus the radius, experiment 15.

In the plots of the average potential for all rows within the screened interval, a straight linear segment was observed close to the contact representing the screen. The true permeability value used was that calculated from the slope of this linear segment—more specifically, from the data from r_w to a radius beyond which the flow outside the screened interval became measurable

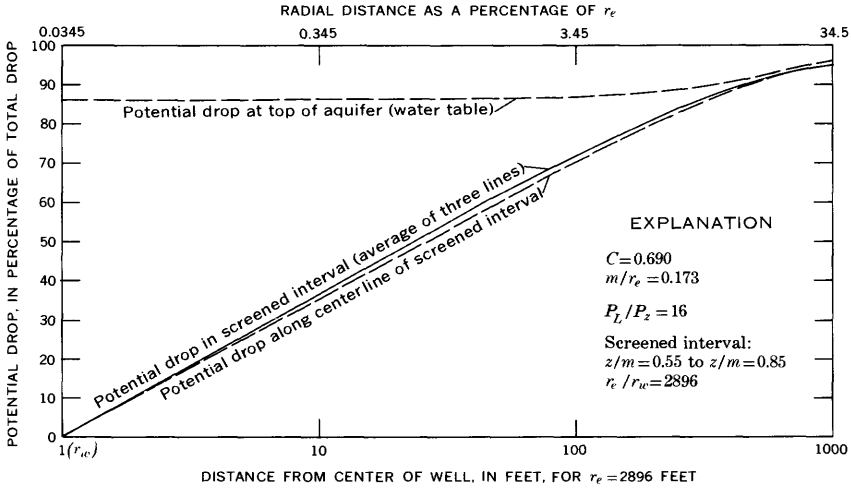

FIGURE 5.—Percentage of total potential drop within a given radius versus the radius, experiment 1.

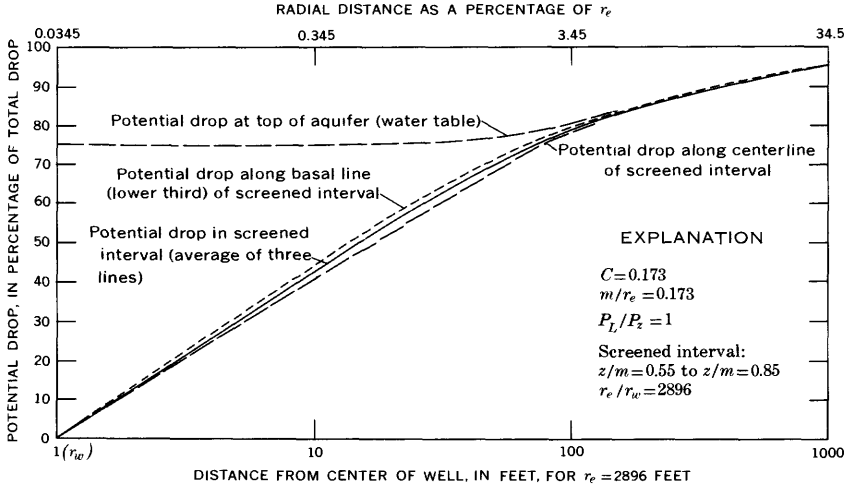

FIGURE 6.—Percentage of total potential drop within a given radius versus the radius, experiment 6.

or exceeded about 0.5 percent of the total flow. Permeability values calculated from data taken elsewhere in the network were compared with this value to determine errors.

The error in determining the permeability from different pairs of observation wells or piezometers is given in table 5. All the data are given for aquifers of specific dimensions, and observation-

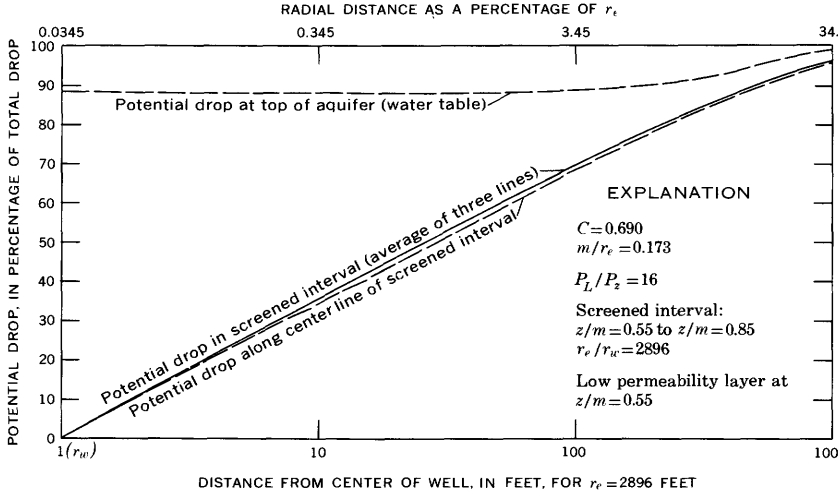

FIGURE 7.—Percentage of total potential drop within a given radius versus the radius, experiment 2.

well spacings are given in feet rather than in dimensionless form. The results can be applied to any combination of dimensions which will give the same flow-net constant, r_w/r_e ratio, and screened interval as the experiment listed, provided that the observation-well spacings are kept in the same r/r_e ratio as in in table 4. The table indicates that if the near observation well is within a foot of the pumped well (for example, in the gravel pack) and the far observation wells are not more than 100 feet from the pumped well, the error in determining the permeability will be less than 10 percent for almost any aquifer parameters. For anisotropies common in the Indus plains, 15:1 to 90:1, the error will be much less, and wells up to a distance of 200 feet can be used. If the near observation well is at a distance of 100 feet from the pumped well and the far observation well is 300 or 400 feet from the pumped well, the errors in permeability at these anisotropies will range between 10 and 30 percent. Thus the permeabilities reported by Bennett, Rehman, Sheikh, and Ali (1967) probably contain errors in this range.

For the pairs of observation wells listed in table 4, screening the entire thickness of the interval apparently gives only slightly better results than screening only part of the interval. Because screening in the upper third of the screened interval seems generally to give results as accurate as those from any other depth, wells of this design have the advantage of lower cost and less chance of failure during drilling and development. The preferred

TABLE 5.—*Percentage of error, due to convergent flow to partially penetrating wells, in calculating permeability from distance-drawdown data*

[See table 1 for data on screen geometries and model constants]

Experiment	Anisotropy P_L/P_s	Depth at which observation well was screened [1]	Percentage of error for indicated pairs of wells (wells given as feet from r_w)							
			1;50	1;100	10;100	10;200	10;300	100;200	100;300	100;400
6	1:1	Same as pumped well	3	8.5	17	31	40	96	117	129
		Center third	5.1	9.9	16	27	38	85	106	115
		Upper third	2.5	8.5	20	33	41	96	117	129
		Lower third	1.7	7.6	28	35	45	106	129	140
7	4:1	Same as pumped well	1.3	3.3	8.7	12	17	34	41	50
		Center third	2.7	4.2	7.1	10	15	29	32	39
		Upper third	.5	2.7	8.7	14	19	34	41	50
7A	8:1	Same as pumped well	.8	2.8	8.3	11.6	15	35	43	52
		Center third	3.6	4.6	5.5	9.2	13	26	35	41
		Upper third	.8	2.8	7.6	11	14	33	41	49
1	16:1	Same as pumped well	.7	1.5	3.7	6.7	13.3	22	26	30
		Center third	3.7	4.3	4.5	5.5	7.4	12	16	24
		Upper third	.5	1.1	2.5	5.8	10.0	22	26	30
		Lower third	−1.3	.0	2.0	4.4	12.3	24	30	37
15	32:1	Same as pumped well (average of two lines)	.6	1.2	2.5	5.5	8.4	19	24	29
8	64:1	Same as pumped well	.0	1.0	1.6	2.6	3.2	10.0	13	15
		Center third	2.2	2.2	2.6	3.2	3.9	4.9	6.7	10
		Upper third	+.6	.0	.0	3.2	4.6	9.6	12	15
1C	16:1	Same as pumped well	1.7	3.7	9	15	20	48	63	80

[1] In comparison with screened interval of test well.

spacing of observation wells in the Indus plains might be one well in the gravel pack (about $r=1$ foot) and one each at 5, 30, 100, 400, and 2,000 feet. If, for reasons of economy, a smaller number are used, the preferred spacing might be gravel pack, 30, and 100 feet.

To determine vertical movement of water from the water table to the screened interval, vertical permeabilities, and specific yield (Bennett and others, 1967), observations on the water table are desirable. The decline in potential along the top of the grid (or the water table) has also been plotted in figures 3–7. Expressed as a percentage of the total drop between r_e and r_w, the drop in the water table near r_w ranges from about 10 to 25 percent. The water table in the vicinity of r_w is flat, and the radius to which the flat part extends varies with anisotropy. In figure 3, the radius is flat for about 200 feet. This flatness indicates that velocity components at the water table in this interval are predominantly vertical, a condition arising from the location of the screen at some depth below the free surface.

To test whether the analog model results were realistic, data from several pumping tests in the Indus plains were plotted in figures 8–11 in the same manner as the analog results. The similarity to the profiles in figures 3–7 is obvious; for example, the data plotted in figure 8, which represents the pumping test on Bari Doab test well 8 (Bennett and others, 1967) compare very closely with the analog data in figure 5.

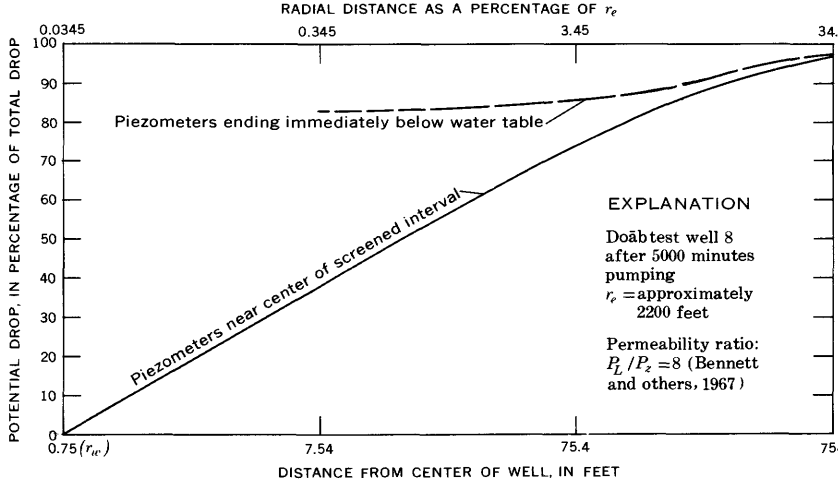

FIGURE 8.—Percentage of total potential drop within a given radius versus the radius, Bari Doab test well 8.

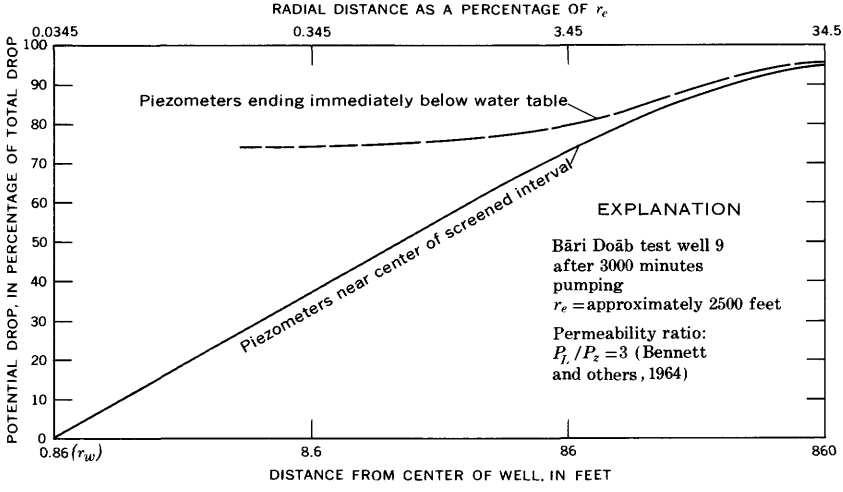

FIGURE 9.—Percentage of total potential drop within a given radius versus the radius, Bari Doab test well 9.

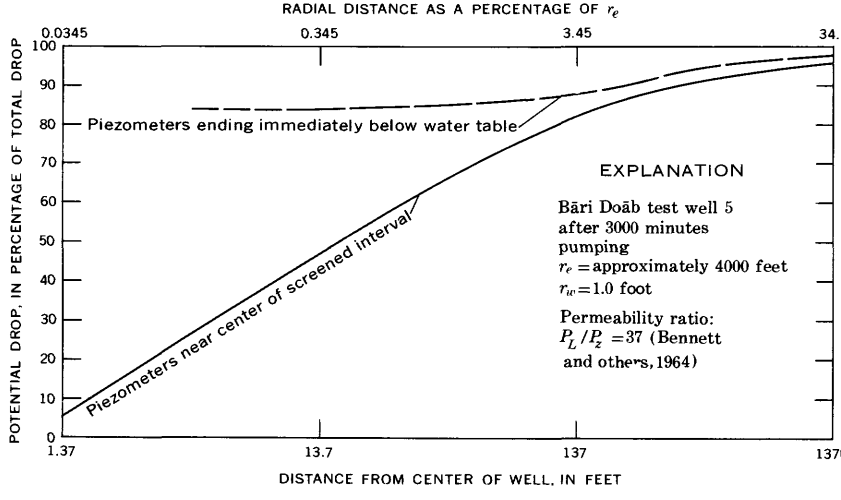

FIGURE 10.—Percentage of total potential drop within a given radius versus the radius, Bari Doab test well 5.

TRAVELTIME OF WATER

In a large part of the Punjab, the aquifer contains brackish water at depths ranging from just below the water table to more than 1,000 feet. Tapping the overlying fresh water without producing excessive quantities of the brackish water is a significant problem of ground-water development in the region.

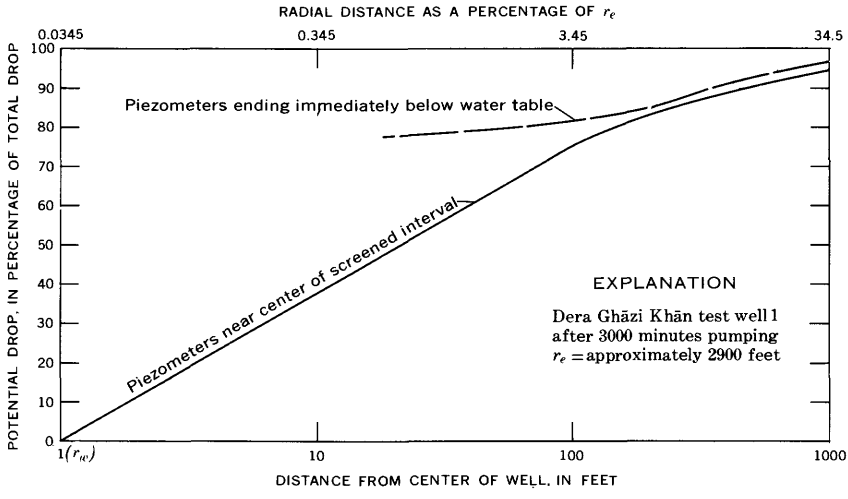

FIGURE 11.—Percentage of total potential drop within a given radius versus the radius, Dera Ghazi Khan test well 1.

The irrigation plan in the Punjab involves the continued importation of all available surface-water supplies and the use of supplemental irrigation from ground water. In many areas, groundwater pumpage may equal or exceed the surface-water diversions reaching farm laterals. In the past, there has been little artificial export of water; most water loss from the system has been, and continues to be, through evapotranspiration and consumptive use by crops. Under this system, the total dissolved solids in the ground water must increase continuously. In the future, moreover, leaching of saline soils in the reclamation process will further add to the salinity. The effects of these processes on the quality of the pumped ground water constitute another important problem of ground-water development.

In these water-quality problems, traveltime of water through the aquifer is of some interest, and the flow nets can readily be used to compute both relative and absolute traveltimes. The average velocity through a stream tube carrying a discharge q, at a point where the cross-sectional area of the tube is A, is given by

$$v=\frac{q}{Ap}, \tag{8}$$

where p is the porosity of the aquifer. If the symbol s is used to represent distance from the well screen along the centerline of a stream tube, the time required for a particle of water to move a

small distance, Δs, along the tube is given by

$$\Delta t = \frac{\Delta s}{v} = \frac{pA\Delta s}{q}. \tag{9}$$

The quantity $A\Delta s$ is simply the volume of the stream tube through which the time of travel is required. In the flow patterns on plate 1, the cross-sectional area A of a stream tube is given by $2\pi rb$, where r is the radius to the point at which the area is taken and b is the width of the tube normal to the direction of flow at this point. The product rb can be determined and plotted as a function of s along any stream tube by simply making the appropriate measurements on the flow net. Because this product is a function of s, the total time of flow along a given stream tube from a distance D to the well screen is given by

$$t_D = \frac{2\pi p}{q}\int_0^D (rb)\, ds\,. \tag{10}$$

The integral in equation 10 is the area under a plot of the product rb from $s=0$ to $s=D$. The quantity $2\pi\int_0^D (rb)\,ds$ is the total volume of the stream tube between the cross section at D and the well screen. For each of the 10 stream tubes in a given flow net, the discharge q is the same; that is, q is equal to $0.1Q$, where Q is the well discharge. The porosity p may also be considered the same for each stream tube. Thus the integral of equation 10, the area under the plot of rb versus s, measures the relative time of travel from a given point to the screen (traveltime from that point relative to traveltime from any other point in the flow net).

Relative traveltimes from the water table to the screen along each of the 10 stream tubes were determined for the flow nets of experiments 1, 6, and 8. In figure 12, for each of these three experiments, the relative traveltime for each stream tube is plotted against the mean stream-function value for that tube. The relative traveltimes in different experiments can be compared only if the well discharge Q is considered the same for each. (As noted previously, Q differs in different flow nets if the potential drop or drawdown is the same.)

Relative traveltimes for water particles originating at various distances from the screen in selected stream tubes are compared in table 6, where the points of origin are at the water-table surface and at radial distances of 0.50 r_e and 0.25 r_e in each stream tube. For values given in table 6 and figure 12, m is equal to 500, and r_e is equal to 2,896. For these values of m and r_e, the figures given in the table and taken from the graph are multiplied by $2\pi 10^7$ to

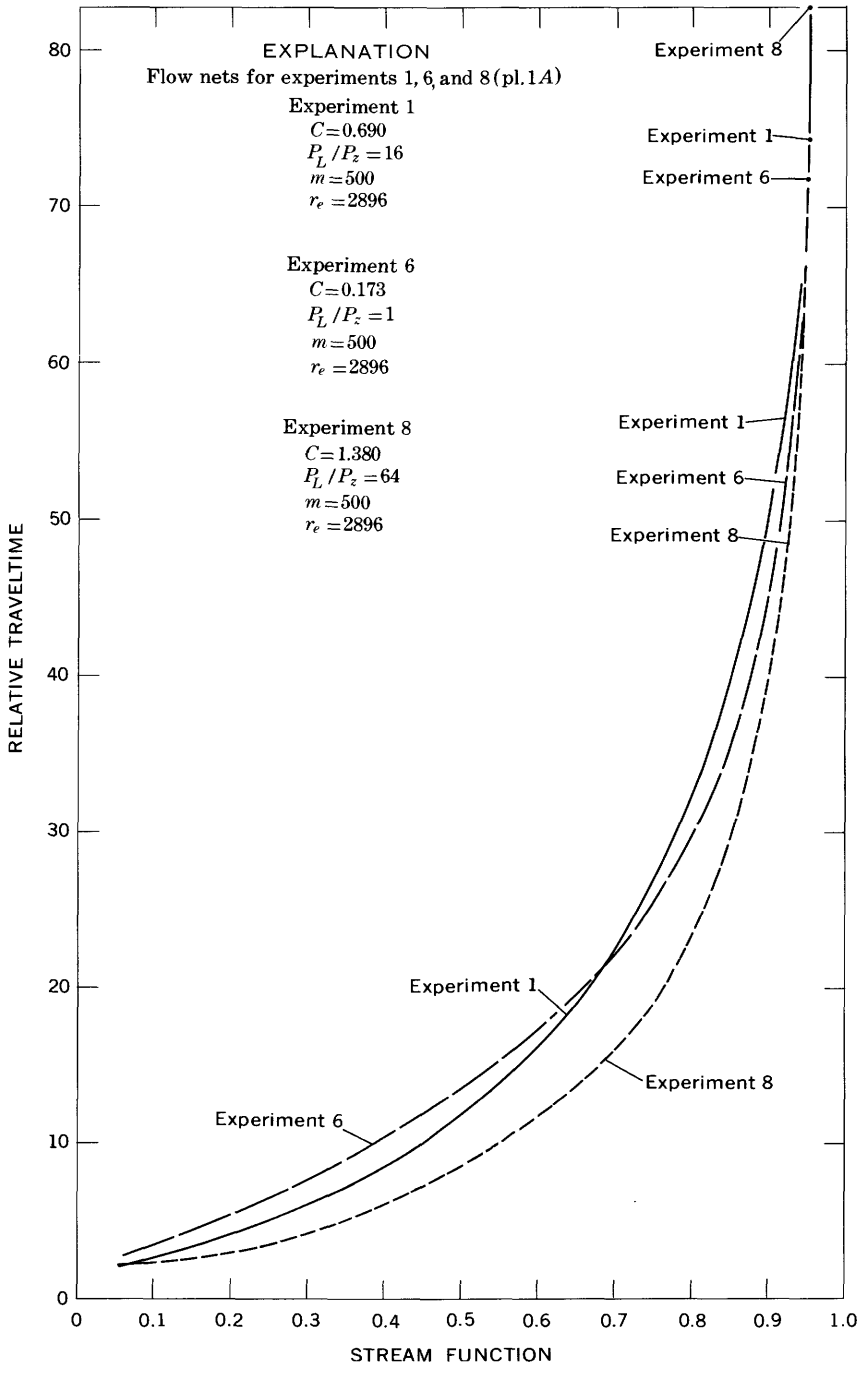

FIGURE 12.—Relative traveltime for water particles to reach the pumped well from the water table via different stream tubes versus mean stream-function values for the stream tubes (traveltime arbitrarily taken as 10 time units for a water particle originating at the water table on the 0.45 streamline in experiment 1).

TABLE 6.—*Relative traveltimes in selected stream tubes*

Experiment	Stream tube (identified by stream functions of bounding surfaces)	Relative traveltime for particle of water originating at—		
		0.25 r_e	0.50 r_e	Water table
8	0.60–0.70	0.52	3.4	14.4
	.70– .80	.52	3.4	18.2
	.80– .90	.72	5.2	29.0
	.90– .99	3.00	15.0	83.0
1	.60– .70	.71	3.76	22.0
	.70– .80	.96	5.47	28.5
	.80– .90	1.46	7.73	37.8
	.90– .99	3.84	12.4	74.2
6	.60– .70	1.15	5.30	20.7
	.70– .80	1.30	5.95	26.7
	.80– .90	1.40	6.05	35.6
	.90– .99	1.60	6.30	71.8

obtain the stream-tube volume between r_w and the applicable point of origin (0.25 r_e, 0.50 r_e, or the water table). This stream-tube volume may be substituted for the term $2\pi\int_0^D (rb)\,ds$ in equation 10; therefore, the actual traveltime is given by

$$t=\frac{pV_{st}}{0.1Q}, \tag{11}$$

where V_{st} is the stream-tube volume from r_w to the point of origin of the water particle. The traveltime for any other combination of m and r_e which is compatible with the flow-net constant, screened interval, and ratio of r_w to r_e in experiments 1, 6, and 8 is computed by multiplying the result as calculated previously by the factor $m_l r_{el}^2/[500(2{,}896)^2]$, where m_l and r_{el} refer to the system for which traveltime is being calculated.

As an example of traveltime calculation, consider a system in which m is 500 feet, r_e is 2,896 feet, well discharge is 4 cubic feet per second, porosity is 0.20, anisotropy (P_L/P_z) is 64, r_w is 1 foot, and the screen extends from 75 to 175 feet below the water table. This screen geometry and anisotropy are represented by experiment 8. The time required for a fluid particle to move from 0.25 r_e to r_w through the stream tube bounded by the stream functions 0.70 and 0.80 is given by $t=(0.52\times 2\pi\times 10^7\times 0.2$ cu ft)/(0.1×4 cu ft sec×86,400 sec day) =190 days.

If the calculation is applied to an aquifer for which P_L/P_z is 32, m is 1,000 feet, r_e is 4,096, r_w is 1.4 feet, and the screen extends from 150 to 350 feet below the water table, the above traveltime is multiplied by $[1{,}000\times(4{,}096)^2]/[500\times(2{,}896)^2]$. This yields a traveltime of 760 days for a particle of fluid to move from 0.25 r_e to r_w along the 0.70–0.80 stream tube.

Traveltime calculations similar to the previous ones are used in conjunction with assumptions or field information on water

quality, soil salinity, and so on, to estimate the way in which the quality of pumped irrigation water will change with time.

SUMMARY AND CONCLUSIONS

The flow nets derived from the analog study provide useful information about flow patterns associated with various screen settings, anisotropies, and occurrences of clay.

The errors in permeability determination by the distance-drawdown procedure—flow thickness is equal to the screened interval—vary according to the spacing of the observation wells that are employed. The analog results indicate that the permeability results reported by Bennett, Rehman, Sheikh, and Ali (1967) may contain errors in the range of 10–30 percent.

Traveltimes for water particles moving through various stream tubes can be readily calculated from the analog results. These traveltimes vary with the stream tube, point of origin of the particle within the tube, anisotropy, screen setting, radius of influence, and other characteristics of the flow problem. Determinations of traveltime have potential value in the solution of problems relating to the variation of chemical quality of the pumped water with time.

REFERENCES

Arif, A. H., 1966, Analysis of selected tests of aquifer characteristics, West Pakistan: Water and Power Devel. Authority, Water and Soils Inv. Div., Tech. Paper 13, 79 p.

Bennett, G. D., Rehman, A., Sheikh, I. A., and Ali, Sabir, 1967, Analysis of aquifer tests in the Punjab region of West Pakistan: U.S. Geol. Survey Water-Supply Paper 1608–G, 56 p.

Chaudhari, A. R., 1966, Analysis of hydrologic performance tests in unconfined aquifers: Water and Power Devel. Authority, Water and Soils Inv. Div., Tech. Paper 14, 90 p.

Greenman, D. W., Swarzenski, W. V., and Bennett, G. D., 1967, The groundwater hydrology of the Punjab, West Pakistan, with emphasis on problems caused by canal irrigation: U.S. Geol. Survey Water-Supply Paper 1608–H, 66 p.

Stallman, R. W., 1963, Electric analog of three-dimensional flow to wells and its application to unconfined aquifers: U.S. Geol. Survey Water-Supply Paper 1536–H, 38 p.

☆U.S. GOVERNMENT PRINTING OFFICE: 1972 O—448–883